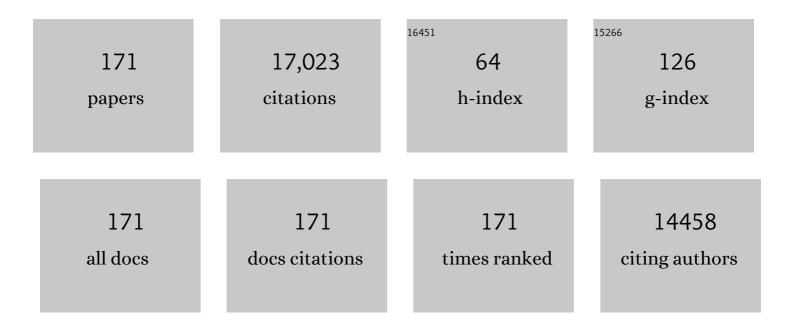
Baoliang Chen

List of Publications by Year in descending order

Source: https://exaly.com/author-pdf/1531064/publications.pdf Version: 2024-02-01



#	Article	IF	CITATIONS
1	Transitional Adsorption and Partition of Nonpolar and Polar Aromatic Contaminants by Biochars of Pine Needles with Different Pyrolytic Temperatures. Environmental Science & Technology, 2008, 42, 5137-5143.	10.0	1,446
2	A novel magnetic biochar efficiently sorbs organic pollutants and phosphate. Bioresource Technology, 2011, 102, 716-723.	9.6	810
3	Adsorption of Polycyclic Aromatic Hydrocarbons by Graphene and Graphene Oxide Nanosheets. Environmental Science & Technology, 2014, 48, 4817-4825.	10.0	668
4	Effects and mechanisms of biochar-microbe interactions in soil improvement and pollution remediation: A review. Environmental Pollution, 2017, 227, 98-115.	7.5	634
5	Insight into Multiple and Multilevel Structures of Biochars and Their Potential Environmental Applications: A Critical Review. Environmental Science & Technology, 2018, 52, 5027-5047.	10.0	593
6	Sorption of naphthalene and 1-naphthol by biochars of orange peels with different pyrolytic temperatures. Chemosphere, 2009, 76, 127-133.	8.2	506
7	Environmental Applications of Three-Dimensional Graphene-Based Macrostructures: Adsorption, Transformation, and Detection. Environmental Science & Technology, 2015, 49, 67-84.	10.0	491
8	Investigation of thermodynamic parameters in the pyrolysis conversion of biomass and manure to biochars using thermogravimetric analysis. Bioresource Technology, 2013, 146, 485-493.	9.6	421
9	Transformation, Morphology, and Dissolution of Silicon and Carbon in Rice Straw-Derived Biochars under Different Pyrolytic Temperatures. Environmental Science & Technology, 2014, 48, 3411-3419.	10.0	406
10	Macroscopic and Spectroscopic Investigations of the Adsorption of Nitroaromatic Compounds on Graphene Oxide, Reduced Graphene Oxide, and Graphene Nanosheets. Environmental Science & Technology, 2015, 49, 6181-6189.	10.0	321
11	Aromatic and Hydrophobic Surfaces of Wood-derived Biochar Enhance Perchlorate Adsorption via Hydrogen Bonding to Oxygen-containing Organic Groups. Environmental Science & Technology, 2014, 48, 279-288.	10.0	315
12	Adsorption and coadsorption of organic pollutants and a heavy metal by graphene oxide and reduced graphene materials. Chemical Engineering Journal, 2015, 281, 379-388.	12.7	301
13	Quantification of Chemical States, Dissociation Constants and Contents of Oxygen-containing Groups on the Surface of Biochars Produced at Different Temperatures. Environmental Science & Technology, 2015, 49, 309-317.	10.0	277
14	Fast and Slow Rates of Naphthalene Sorption to Biochars Produced at Different Temperatures. Environmental Science & Technology, 2012, 46, 11104-11111.	10.0	269
15	Aggregation, Adsorption, and Morphological Transformation of Graphene Oxide in Aqueous Solutions Containing Different Metal Cations. Environmental Science & Technology, 2016, 50, 11066-11075.	10.0	265
16	Sulfonated Graphene Nanosheets as a Superb Adsorbent for Various Environmental Pollutants in Water. Environmental Science & Technology, 2015, 49, 7364-7372.	10.0	255
17	Interactions of Aluminum with Biochars and Oxidized Biochars: Implications for the Biochar Aging Process. Journal of Agricultural and Food Chemistry, 2014, 62, 373-380.	5.2	249
18	Distributions of polycyclic aromatic hydrocarbons in surface waters, sediments and soils of Hangzhou City, China. Water Research, 2004, 38, 3558-3568.	11.3	248

#	Article	IF	CITATIONS
19	Sorption of Poly- and Perfluoroalkyl Substances (PFASs) Relevant to Aqueous Film-Forming Foam (AFFF)-Impacted Groundwater by Biochars and Activated Carbon. Environmental Science & Technology, 2017, 51, 6342-6351.	10.0	239
20	Synthesis, decoration and properties of three-dimensional graphene-based macrostructures: A review. Chemical Engineering Journal, 2015, 264, 753-771.	12.7	223
21	Sorption of Polar and Nonpolar Aromatic Organic Contaminants by Plant Cuticular Materials:  Role of Polarity and Accessibility. Environmental Science & Technology, 2005, 39, 6138-6146.	10.0	222
22	Enhanced sorption of polycyclic aromatic hydrocarbons by soil amended with biochar. Journal of Soils and Sediments, 2011, 11, 62-71.	3.0	221
23	Sorption of Phenol,p-Nitrophenol, and Aniline to Dual-Cation Organobentonites from Water. Environmental Science & Technology, 2000, 34, 468-475.	10.0	206
24	Enhanced bioremediation of PAH-contaminated soil by immobilized bacteria with plant residue and biochar as carriers. Journal of Soils and Sediments, 2012, 12, 1350-1359.	3.0	179
25	Insights on the Molecular Mechanism for the Recalcitrance of Biochars: Interactive Effects of Carbon and Silicon Components. Environmental Science & Technology, 2014, 48, 9103-9112.	10.0	179
26	Structural characteristics of biochar-graphene nanosheet composites and their adsorption performance for phthalic acid esters. Chemical Engineering Journal, 2017, 319, 9-20.	12.7	174
27	Wrinkles and Folds of Activated Graphene Nanosheets as Fast and Efficient Adsorptive Sites for Hydrophobic Organic Contaminants. Environmental Science & Technology, 2016, 50, 3798-3808.	10.0	173
28	A Direct Observation of the Fine Aromatic Clusters and Molecular Structures of Biochars. Environmental Science & Technology, 2017, 51, 5473-5482.	10.0	173
29	Simultaneously Tuning Band Structure and Oxygen Reduction Pathway toward Highâ€Efficient Photocatalytic Hydrogen Peroxide Production Using Cyanoâ€Rich Graphitic Carbon Nitride. Advanced Functional Materials, 2021, 31, 2105731.	14.9	167
30	Self-assembly of graphene oxide aerogels by layered double hydroxides cross-linking and their application in water purification. Journal of Materials Chemistry A, 2014, 2, 8941-8951.	10.3	163
31	H/C atomic ratio as a smart linkage between pyrolytic temperatures, aromatic clusters and sorption properties of biochars derived from diverse precursory materials. Scientific Reports, 2016, 6, 22644.	3.3	149
32	Porous PVdF/GO Nanofibrous Membranes for Selective Separation and Recycling of Charged Organic Dyes from Water. Environmental Science & Technology, 2018, 52, 4265-4274.	10.0	144
33	Effective Alleviation of Aluminum Phytotoxicity by Manure-Derived Biochar. Environmental Science & Technology, 2013, 47, 2737-2745.	10.0	140
34	Bisolute Sorption and Thermodynamic Behavior of Organic Pollutants to Biomass-derived Biochars at Two Pyrolytic Temperatures. Environmental Science & Technology, 2012, 46, 12476-12483.	10.0	139
35	Sorption Behavior of p-Nitrophenol on the Interface between Anionâ^ Cation Organobentonite and Water. Environmental Science & Technology, 2000, 34, 2997-3002.	10.0	133
36	Interactions of Organic Contaminants with Mineral-Adsorbed Surfactants. Environmental Science & Technology, 2003, 37, 4001-4006.	10.0	133

#	Article	IF	CITATIONS
37	Configurations of the Bentonite-Sorbed Myristylpyridinium Cation and Their Influences on the Uptake of Organic Compounds. Environmental Science & Technology, 2005, 39, 6093-6100.	10.0	130
38	Self-Assembled Nano-FeO(OH)/Reduced Graphene Oxide Aerogel as a Reusable Catalyst for Photo-Fenton Degradation of Phenolic Organics. Environmental Science & Technology, 2018, 52, 7043-7053.	10.0	121
39	Biosorption and biodegradation of polycyclic aromatic hydrocarbons in aqueous solutions by a consortium of white-rot fungi. Journal of Hazardous Materials, 2010, 179, 845-851.	12.4	120
40	Solubilization and biodegradation of phenanthrene in mixed anionic–nonionic surfactant solutions. Chemosphere, 2005, 58, 33-40.	8.2	118
41	Application of biochar-based materials in environmental remediation: from multi-level structures to specific devices. Biochar, 2020, 2, 1-31.	12.6	118
42	Stable graphene oxide/poly(ethyleneimine) 3D aerogel with tunable surface charge for high performance selective removal of ionic dyes from water. Chemical Engineering Journal, 2018, 334, 1119-1127.	12.7	116
43	Removal of polycyclic aromatic hydrocarbons from aqueous solution using plant residue materials as a biosorbent. Journal of Hazardous Materials, 2011, 188, 436-442.	12.4	105
44	In situ photochemical fabrication of CdS/g-C3N4 nanocomposites with high performance for hydrogen evolution under visible light. Applied Catalysis B: Environmental, 2019, 256, 117848.	20.2	105
45	Overall photosynthesis of H2O2 by an inorganic semiconductor. Nature Communications, 2022, 13, 1034.	12.8	105
46	Linking hydrophobicity of biochar to the water repellency and water holding capacity of biochar-amended soil. Environmental Pollution, 2019, 253, 779-789.	7.5	103
47	Application of graphene-based materials in water purification: from the nanoscale to specific devices. Environmental Science: Nano, 2018, 5, 1264-1297.	4.3	102
48	Aggregation Kinetics and Self-Assembly Mechanisms of Graphene Quantum Dots in Aqueous Solutions: Cooperative Effects of pH and Electrolytes. Environmental Science & Technology, 2017, 51, 1364-1376.	10.0	97
49	Synergistic effects of 2D graphene oxide nanosheets and 1D carbon nanotubes in the constructed 3D carbon aerogel for high performance pollutant removal. Chemical Engineering Journal, 2017, 314, 336-346.	12.7	93
50	Dual Role of Biochars as Adsorbents for Aluminum: The Effects of Oxygen-Containing Organic Components and the Scattering of Silicate Particles. Environmental Science & Technology, 2013, 47, 130719140420001.	10.0	92
51	Environmental Effects of Silicon within Biochar (Sichar) and Carbon–Silicon Coupling Mechanisms: A Critical Review. Environmental Science & Technology, 2019, 53, 13570-13582.	10.0	91
52	Enhanced sorption of polycyclic aromatic hydrocarbons from aqueous solution by modified pine bark. Bioresource Technology, 2010, 101, 7307-7313.	9.6	88
53	Competitive adsorption of cadmium and aluminum onto fresh and oxidized biochars during aging processes. Journal of Soils and Sediments, 2015, 15, 1130-1138.	3.0	88
54	Nanocomposite Membrane with Polyethylenimine-Grafted Graphene Oxide as a Novel Additive to Enhance Pollutant Filtration Performance. Environmental Science & Technology, 2018, 52, 5920-5930.	10.0	88

#	Article	IF	CITATIONS
55	Durable Superhydrophobic/Superoleophilic Graphene-Based Foam for High-Efficiency Oil Spill Cleanups and Recovery. Environmental Science & Technology, 2019, 53, 1509-1517.	10.0	85
56	Understanding the mechanisms of soil water repellency from nanoscale to ecosystem scale: a review. Journal of Soils and Sediments, 2019, 19, 171-185.	3.0	81
57	Organic carbon and inorganic silicon speciation in rice-bran-derived biochars affect its capacity to adsorb cadmium in solution. Journal of Soils and Sediments, 2015, 15, 60-70.	3.0	79
58	Pollution survey of polycyclic aromatic hydrocarbons in surface water of Hangzhou, China. Chemosphere, 2004, 56, 1085-1095.	8.2	77
59	Adsorption of perchlorate onto raw and oxidized carbon nanotubes in aqueous solution. Carbon, 2012, 50, 2209-2219.	10.3	77
60	Removal of polycyclic aromatic hydrocarbons from aqueous solution by raw and modified plant residue materials as biosorbents. Journal of Environmental Sciences, 2014, 26, 737-748.	6.1	76
61	Adsorption and desorption of phthalic acid esters on graphene oxide and reduced graphene oxide as affected by humic acid. Environmental Pollution, 2018, 232, 505-513.	7.5	75
62	Graphene-coated materials using silica particles as a framework for highly efficient removal of aromatic pollutants in water. Scientific Reports, 2015, 5, 11641.	3.3	72
63	Covalently cross-linked graphene oxide aerogel with stable structure for high-efficiency water purification. Chemical Engineering Journal, 2018, 354, 896-904.	12.7	68
64	Size effects of graphene oxide nanosheets on the construction of three-dimensional graphene-based macrostructures as adsorbents. Journal of Materials Chemistry A, 2016, 4, 12106-12118.	10.3	66
65	Direct Observation, Molecular Structure, and Location of Oxidation Debris on Graphene Oxide Nanosheets. Environmental Science & Technology, 2016, 50, 8568-8577.	10.0	64
66	Sugar Cane-Converted Graphene-like Material for the Superhigh Adsorption of Organic Pollutants from Water via Coassembly Mechanisms. Environmental Science & Technology, 2017, 51, 12644-12652.	10.0	63
67	Enhanced bisphenol A removal from stormwater in biochar-amended biofilters: Combined with batch sorption and fixed-bed column studies. Environmental Pollution, 2018, 243, 1539-1549.	7.5	61
68	pH-dependent sorption of sulfonamide antibiotics onto biochars: Sorption mechanisms and modeling. Environmental Pollution, 2019, 248, 48-56.	7.5	61
69	A nonradical reaction-dominated phenol degradation with peroxydisulfate catalyzed by nitrogen-doped graphene. Science of the Total Environment, 2019, 667, 287-296.	8.0	60
70	Low-pressure driven electrospun membrane with tuned surface charge for efficient removal of polystyrene nanoplastics from water. Journal of Membrane Science, 2020, 614, 118470.	8.2	59
71	Perchlorate uptake and molecular mechanisms by magnesium/aluminum carbonate layered double hydroxides and the calcined layered double hydroxides. Chemical Engineering Journal, 2014, 237, 38-46.	12.7	58
72	Facile fabrication of stable monolayer and few-layer graphene nanosheets as superior sorbents for persistent aromatic pollutant management in water. Journal of Materials Chemistry A, 2014, 2, 18219-18224.	10.3	57

#	Article	IF	CITATIONS
73	Organic Pollutant Clustered in the Plant Cuticular Membranes: Visualizing the Distribution of Phenanthrene in Leaf Cuticle Using Two-Photon Confocal Scanning Laser Microscopy. Environmental Science & Technology, 2014, 48, 4774-4781.	10.0	56
74	Effects of biochar nanoparticles on seed germination and seedling growth. Environmental Pollution, 2020, 256, 113409.	7.5	56
75	Role of the Extractable Lipids and Polymeric Lipids in Sorption of Organic Contaminants onto Plant Cuticles. Environmental Science & Technology, 2008, 42, 1517-1523.	10.0	55
76	Sorption and Conformational Characteristics of Reconstituted Plant Cuticular Waxes on Montmorillonite. Environmental Science & amp; Technology, 2005, 39, 8315-8323.	10.0	54
77	Novel Alleviation Mechanisms of Aluminum Phytotoxicity via Released Biosilicon from Rice Straw-Derived Biochars. Scientific Reports, 2016, 6, 29346.	3.3	52
78	Driving forces linking microbial community structure and functions to enhanced carbon stability in biochar-amended soil. Environment International, 2019, 133, 105211.	10.0	49
79	Resolution of Adsorption and Partition Components of Organic Compounds on Black Carbons. Environmental Science & Technology, 2015, 49, 9116-9123.	10.0	48
80	Magnetic biochar supported α-MnO2 nanorod for adsorption enhanced degradation of 4-chlorophenol via activation of peroxydisulfate. Science of the Total Environment, 2020, 724, 138278.	8.0	45
81	Biosorption and biodegradation of phenanthrene and pyrene in sterilized and unsterilized soil slurry systems stimulated by Phanerochaete chrysosporium. Journal of Hazardous Materials, 2012, 229-230, 159-169.	12.4	44
82	Microstructure of organo-bentonites in water and the effect of steric hindrance on the uptake of organic compounds. Clays and Clay Minerals, 2008, 56, 144-154.	1.3	43
83	Single-solute and bi-solute sorption of phenanthrene and pyrene onto pine needle cuticular fractions. Environmental Pollution, 2010, 158, 2478-2484.	7.5	43
84	Metal composition of layered double hydroxides (LDHs) regulating ClOâ^'4 adsorption to calcined LDHs via the memory effect and hydrogen bonding. Journal of Environmental Sciences, 2014, 26, 493-501.	6.1	43
85	Scalable graphene oxide membranes with tunable water channels and stability for ion rejection. Environmental Science: Nano, 2019, 6, 904-915.	4.3	43
86	Membranes prepared from graphene-based nanomaterials for sustainable applications: a review. Environmental Science: Nano, 2017, 4, 2267-2285.	4.3	42
87	Novel insights into effects of silicon-rich biochar (Sichar) amendment on cadmium uptake, translocation and accumulation in rice plants. Environmental Pollution, 2020, 265, 114772.	7.5	42
88	Efficient removal and mechanisms of water soluble aromatic contaminants by a reduced-charge bentonite modified with benzyltrimethylammonium cation. Chemosphere, 2008, 70, 1987-1994.	8.2	41
89	Biochar Impacts on Soil Silicon Dissolution Kinetics and their Interaction Mechanisms. Scientific Reports, 2018, 8, 8040.	3.3	39
90	Biosorption and biodegradation of polycyclic aromatic hydrocarbons by Phanerochaete chrysosporium in aqueous solution. Science Bulletin, 2013, 58, 613-621.	1.7	38

#	Article	IF	CITATIONS
91	Water clusters contributed to molecular interactions of ionizable organic pollutants with aromatized biochar via π-PAHB: Sorption experiments and DFT calculations. Environmental Pollution, 2018, 240, 342-352.	7.5	38
92	Correlations of nonlinear sorption of organic solutes with soil/sediment physicochemical properties. Chemosphere, 2005, 61, 116-128.	8.2	37
93	Cobalt (II)-based openâ€framework systems constructed on g-C3N4 for extraordinary enhancing photocatalytic hydrogen evolution. Applied Catalysis B: Environmental, 2020, 277, 119207.	20.2	37
94	Phenanthrene Sorption by Fruit Cuticles and Potato Periderm with Different Compositional Characteristics. Journal of Agricultural and Food Chemistry, 2009, 57, 637-644.	5.2	36
95	Synergistic oxytetracycline adsorption and peroxydisulfate-driven oxidation on nitrogen and sulfur co-doped porous carbon spheres. Journal of Hazardous Materials, 2022, 424, 127444.	12.4	36
96	Dependence of Plant Uptake and Diffusion of Polycyclic Aromatic Hydrocarbons on the Leaf Surface Morphology and Micro-structures of Cuticular Waxes. Scientific Reports, 2017, 7, 46235.	3.3	33
97	Bimetal organic framework/graphene oxide derived magnetic porous composite catalyst for peroxymonosulfate activation in fast organic pollutant degradation. Journal of Hazardous Materials, 2021, 419, 126427.	12.4	33
98	Role of Suberin, Suberan, and Hemicellulose in Phenanthrene Sorption by Root Tissue Fractions of Switchgrass (<i>Panicum virgatum</i>) Seedlings. Environmental Science & Technology, 2009, 43, 4130-4136.	10.0	32
99	Biochar composite membrane for high performance pollutant management: Fabrication, structural characteristics and synergistic mechanisms. Environmental Pollution, 2018, 233, 1013-1023.	7.5	32
100	Enhanced Microbial Ferrihydrite Reduction by Pyrogenic Carbon: Impact of Graphitic Structures. Environmental Science & Technology, 2022, 56, 239-250.	10.0	31
101	Sorption characteristics and mechanisms of organic contaminant to carbonaceous biosorbents in aqueous solution. Science in China Series B: Chemistry, 2008, 51, 464-472.	0.8	30
102	Enhanced sorption of naphthalene and nitroaromatic compounds to bentonite by potassium and cetyltrimethylammonium cations. Journal of Hazardous Materials, 2008, 158, 116-123.	12.4	30
103	Interaction mechanisms of organic contaminants with burned straw ash charcoal. Journal of Environmental Sciences, 2010, 22, 1586-1594.	6.1	30
104	Stable Graphene-Based Membrane with pH-Responsive Gates for Advanced Molecular Separation. Environmental Science & Technology, 2019, 53, 10398-10407.	10.0	30
105	Effects of biochar amendment on the soil silicon cycle in a soil-rice ecosystem. Environmental Pollution, 2019, 248, 823-833.	7.5	30
106	Facile synthesis of porous CoFe2O4/graphene aerogel for catalyzing efficient removal of organic pollutants. Science of the Total Environment, 2021, 775, 143398.	8.0	30
107	Reduction and removal of Cr(VI) in water using biosynthesized palladium nanoparticles loaded Shewanella oneidensis MR-1. Science of the Total Environment, 2022, 805, 150336.	8.0	29
108	Microfluidics as an Emerging Platform for Exploring Soil Environmental Processes: A Critical Review. Environmental Science & Technology, 2022, 56, 711-731.	10.0	29

#	Article	IF	CITATIONS
109	Effects of compositional heterogeneity and nanoporosity of raw and treated biomass-generated soot on adsorption and absorption of organic contaminants. Environmental Pollution, 2011, 159, 550-556.	7.5	28
110	Reconsideration of heterostructures of biochars: Morphology, particle size, elemental composition, reactivity and toxicity. Environmental Pollution, 2019, 254, 113017.	7.5	28
111	Graphene nanofiltration membrane intercalated with AgNP@g-C3N4 for efficient water purification and photocatalytic self-cleaning performance. Chemical Engineering Journal, 2022, 441, 136089.	12.7	28
112	Uniformly Dispersed Metal Sulfide Nanodots on g-C ₃ N ₄ as Bifunctional Catalysts for High-Efficiency Photocatalytic H ₂ and H ₂ O ₂ Production under Visible-Light Irradiation. Energy & Fuels, 2021, 35, 10746-10755.	5.1	27
113	Adsorptive Characteristics of the Siloxane Surfaces of Reduced-Charge Bentonites Saturated with Tetramethylammonium Cation. Environmental Science & amp; Technology, 2008, 42, 7911-7917.	10.0	26
114	Enhanced dissipation of polycyclic aromatic hydrocarbons in the presence of fresh plant residues and their extracts. Environmental Pollution, 2012, 161, 199-205.	7.5	26
115	A New Insight of Graphene oxide-Fe(III) Complex Photochemical Behaviors under Visible Light Irradiation. Scientific Reports, 2017, 7, 40711.	3.3	26
116	Novel photocatalytic performance of nanocage-like MIL-125-NH ₂ induced by adsorption of phenolic pollutants. Environmental Science: Nano, 2020, 7, 1525-1538.	4.3	26
117	Diel Fluctuation of Extracellular Reactive Oxygen Species Production in the Rhizosphere of Rice. Environmental Science & Technology, 2022, 56, 9075-9082.	10.0	25
118	Tide-Triggered Production of Reactive Oxygen Species in Coastal Soils. Environmental Science & Technology, 2022, 56, 11888-11896.	10.0	25
119	Reduced bioavailability and plant uptake of polycyclic aromatic hydrocarbons from soil slurry amended with biochars pyrolyzed under various temperatures. Environmental Science and Pollution Research, 2018, 25, 16991-17001.	5.3	23
120	Membrane hydrophilicity switching via molecular design and re-construction of the functional additive for enhanced fouling resistance. Journal of Membrane Science, 2019, 588, 117222.	8.2	23
121	Effect of background electrolytes on the adsorption of nitroaromatic compounds onto bentonite. Journal of Environmental Sciences, 2009, 21, 1044-1052.	6.1	21
122	Effect of fulvic acid coating on biochar surface structure and sorption properties towards 4-chlorophenol. Science of the Total Environment, 2019, 691, 595-604.	8.0	21
123	High Sample Throughput LED Reactor for Facile Characterization of the Quantum Yield Spectrum of Photochemically Produced Reactive Intermediates. Environmental Science & Technology, 2021, 55, 16204-16214.	10.0	21
124	Selective Separation Catalysis Membrane for Highly Efficient Water and Soil Decontamination via a Persulfate-Based Advanced Oxidation Process. Environmental Science & Technology, 2022, 56, 3234-3244.	10.0	20
125	Underwater superoleophobic PVA–GO nanofibrous membranes for emulsified oily water purification. Environmental Science: Nano, 2019, 6, 3723-3733.	4.3	19
126	Surfactant Effects on the Affinity of Plant Cuticles with Organic Pollutants. Journal of Agricultural and Food Chemistry, 2009, 57, 3681-3688.	5.2	18

#	Article	IF	CITATIONS
127	Enhanced photocatalytic hydrogen peroxide production at a solid-liquid-air interface via microenvironment engineering. Applied Catalysis B: Environmental, 2022, 305, 121066.	20.2	18
128	Sorption Behavior of Polycyclic Aromatic Hydrocarbons in Soil–Water System Containing Nonionic Surfactant. Environmental Engineering Science, 2004, 21, 263-272.	1.6	16
129	Konjac glucomannan biopolymer as a multifunctional binder to build a solid permeable interface on Na ₃ V ₂ (PO ₄) ₃ /C cathodes for high-performance sodium ion batteries. Journal of Materials Chemistry A, 2021, 9, 9864-9874.	10.3	16
130	Effects of ionizable organic compounds in different species on the sorption of p-nitroaniline to sediment. Water Research, 2005, 39, 281-288.	11.3	15
131	Facile fabrication of crumpled graphene oxide nanosheets and its Platinum nanohybrids for high efficient catalytic activity. Environmental Pollution, 2018, 243, 1810-1817.	7.5	15
132	Designing a Nanoscale Three-phase Electrochemical Pathway to Promote Pt-catalyzed Formaldehyde Oxidation. Nano Letters, 2020, 20, 8719-8724.	9.1	15
133	In situ quantitative determination of the intermolecular attraction between amines and a graphene surface using atomic force microscopy. Journal of Colloid and Interface Science, 2021, 581, 385-395.	9.4	15
134	Biochar-amendment-reduced cotransport of graphene oxide nanoparticles and dimethyl phthalate in saturated porous media. Science of the Total Environment, 2020, 705, 135094.	8.0	14
135	Reduced graphene oxide/TiO2(B) immobilized on nylon membrane with enhanced photocatalytic performance. Science of the Total Environment, 2021, 799, 149370.	8.0	14
136	Enhanced oxidation of benzo[a]pyrene by crude enzyme extracts produced during interspecific fungal interaction of Trametes versicolor and Phanerochaete chrysosporium. Journal of Environmental Sciences, 2012, 24, 1639-1646.	6.1	13
137	Organic Pollutant Penetration through Fruit Polyester Skin: A Modified Three-compartment Diffusion Model. Scientific Reports, 2016, 6, 23554.	3.3	13
138	Facile fabrication of freestanding all-carbon activated carbon membranes for high-performance and universal pollutant management. Journal of Materials Chemistry A, 2017, 5, 20316-20326.	10.3	13
139	Triplex Blue-shifting Hydrogen Bonds of ClO ₄ [–] ···H–C in the Nanointerlayer of Montmorillonite Complexed with Cetyltrimethylammonium Cation from Hydrophilic to Hydrophobic Properties. Environmental Science & Technology, 2013, 47, 11013-11022.	10.0	12
140	Inoculation of soil with an Isoproturon degrading microbial community reduced the pool of "real non-extractable―Isoproturon residues. Ecotoxicology and Environmental Safety, 2018, 149, 182-189.	6.0	12
141	Contribution of enrofloxacin and Cu2+ to the antibiotic resistance of bacterial community in a river biofilm. Environmental Pollution, 2021, 291, 118156.	7.5	12
142	The effect of structural compositions on the biosorption of phenanthrene and pyrene by tea leaf residue fractions as model biosorbents. Environmental Science and Pollution Research, 2014, 21, 3318-3330.	5.3	11
143	Immobilizing 1–3â€ ⁻ nm Ag nanoparticles in reduced graphene oxide aerogel as a high-effective catalyst for reduction of nitroaromatic compounds. Environmental Pollution, 2020, 256, 113405.	7.5	11
144	Nanoscale Profiling of 2D Surface Hydrophobicity Recognition of Environmental Media via AFM Measurements In Situ. Environmental Science & Technology, 2020, 54, 9315-9324.	10.0	11

#	Article	IF	CITATIONS
145	Constructing the Support as a Microreactor and Regenerator for Highly Active and In Situ Regenerative Hydrogenation Catalyst. Advanced Functional Materials, 2021, 31, 2100971.	14.9	11
146	Selectively coupled small Pd nanoparticles on sp2-hybridized domain of graphene-based aerogel with enhanced catalytic activity and stability. Science of the Total Environment, 2021, 771, 145396.	8.0	11
147	Janus Membrane with Bioinspired Heterogeneous Morphology for Efficient Fog Harvesting. ACS ES&T Engineering, 2021, 1, 1217-1226.	7.6	11
148	Self-assembled fungus-biochar composite pellets (FBPs) for enhanced co-sorption-biodegradation towards phenanthrene. Chemosphere, 2022, 286, 131887.	8.2	11
149	High-Flux pH-Responsive Ultrafiltration Membrane for Efficient Nanoparticle Fractionation. ACS Applied Materials & Interfaces, 2021, 13, 56575-56583.	8.0	11
150	Facile fabrication of Shewanella@graphene core-shell material and its enhanced performance in nitrobenzene reduction. Science of the Total Environment, 2019, 658, 324-332.	8.0	10
151	In situ scrutinize the adsorption of sulfamethoxazole in water using AFM force spectroscopy: Molecular adhesion force determination and fractionation. Journal of Hazardous Materials, 2022, 426, 128128.	12.4	10
152	Sorption of chlorophenols onto fruit cuticles and potato periderm. Journal of Environmental Sciences, 2012, 24, 675-681.	6.1	9
153	Effect of culturing temperatures on cadmium phytotoxicity alleviation by biochar. Environmental Science and Pollution Research, 2017, 24, 23843-23849.	5.3	9
154	Applications of atomic force microscopy-based imaging and force spectroscopy in assessing environmental interfacial processes. Critical Reviews in Environmental Science and Technology, 2022, 52, 2421-2452.	12.8	9
155	Adhesion force evolution of protein on the surfaces with varied hydration extent: Quantitative determination via atomic force microscopy. Journal of Colloid and Interface Science, 2022, 608, 255-264.	9.4	9
156	Multilayered graphene oxide membrane with precisely controlled interlayer spacing for separation of molecules with very close molecular weights. Journal of Membrane Science, 2022, 657, 120678.	8.2	8
157	Dual-function ultrafiltration membrane constructed from pure activated carbon particles via facile nanostructure reconstruction for high-efficient water purification. Carbon, 2020, 168, 254-263.	10.3	7
158	Proton uptake behaviors of organic and inorganic matters in biochars prepared under different pyrolytic temperatures. Science of the Total Environment, 2020, 746, 140853.	8.0	6
159	Concurrent enhancement of structure stability and adsorption capacity of freeze-dried graphene oxide aerogels <i>via</i> the removal of oxidation debris nanoparticles on nanosheets. Environmental Science: Nano, 2021, 8, 1000-1009.	4.3	6
160	Biomass Hyaluronic Acid to Construct Highâ€Loading Electrode with Fast Na ⁺ Transport Structure for Na ₃ V ₂ (PO ₄) ₃ Sodiumâ€lon Batteries. Batteries and Supercaps, 2022, 5, .	4.7	6
161	Combined 1 H NMR and LSER study for the compound-specific interactions between organic contaminants and organobentonites. Journal of Colloid and Interface Science, 2015, 460, 119-127.	9.4	5
162	Occurrence and transformation of unknown organochlorines in the wastewater treatment plant using specific Fragment-Based method with LC Q-TOF MS. Water Research, 2022, 216, 118372.	11.3	5

#	Article	IF	CITATIONS
163	Interaction Mechanisms between Biochar and Organic Pollutants. SSSA Special Publication Series, 2015, , 225-257.	0.2	4
164	Ultrathin graphene oxide membrane with constructed tent-shaped structures for efficient and tunable molecular sieving. Environmental Science: Nano, 2020, 7, 2373-2384.	4.3	4
165	Facile nitrogen doping in fungal hyphae-derived biochars via cooperation of microbial culture and pyrolysis for efficient catalytic reduction of 4-nitrophenol. Chemosphere, 2022, 300, 134526.	8.2	4
166	Significance of natural organic matter in nonlinear sorption of 2,4-dichlorophenol onto soils/sediments. Water Resources Research, 2004, 40, .	4.2	3
167	Multiple roles of humic acid in the photogeneration of reactive bromine species using a chemical probe method. Environmental Pollution, 2021, 286, 117658.	7.5	3
168	Environmental transport behaviors of perchlorate as an emerging pollutant and their effects on food safety and health risk. Chinese Science Bulletin, 2013, 58, 2626-2642.	0.7	2
169	Bioinspired photo-responsive membrane enhanced with "light-cleaning―feature for controlled molecule release. Journal of Materials Chemistry B, 2022, 10, 2617-2627.	5.8	2
170	Biochar-based asymmetric membrane for selective removal and oxidation of hydrophobic organic pollutants. Chemosphere, 2022, 300, 134509.	8.2	2
171	Heterogeneous Hydrogenation Catalysts: Constructing the Support as a Microreactor and Regenerator for Highly Active and In Situ Regenerative Hydrogenation Catalyst (Adv. Funct. Mater.) Tj ETQq1 1 C).7 84.3 14 r	gBIT /Overloc